

This document is confidential and is proprietary to the American Chemical Society and its authors. Do not copy or disclose without written permission. If you have received this item in error, notify the sender and delete all copies.

**Computational Investigation of RO₂ + HO₂ and RO₂ + RO₂
Reactions of Monoterpene Derived First-Generation Peroxy
Radicals Leading to Radical Recycling**

Journal:	<i>The Journal of Physical Chemistry</i>
Manuscript ID	jp-2018-09241y.R1
Manuscript Type:	Article
Date Submitted by the Author:	n/a
Complete List of Authors:	Iyer, Siddharth; Helsingin Yliopisto, Department of molecular sciences Reiman, Heidi; Helsingin Yliopisto, Department of Chemistry Møller, Kristian; University of Copenhagen, Department of Chemistry Rissanen, Matti; Helsingin Yliopisto, Physics Kjaergaard, Henrik Grum ; Copenhagen University, Chemistry Kurtén, Theo; Helsingin Yliopisto, Department of Chemistry

SCHOLARONE™
Manuscripts

1
2
3
4
5
6
7 **Computational Investigation of RO₂ + HO₂ and**
8 **RO₂ + RO₂ Reactions of Monoterpene Derived**
9
10
11 **First-Generation Peroxy Radicals Leading to**
12
13
14 **Radical Recycling**
15
16
17
18
19
20

21 Siddharth Iyer,^{*,†} Heidi Reiman,[‡] Kristian H. Møller,[¶] Matti P. Rissanen,[§] Henrik
22 G. Kjaergaard,[¶] and Theo Kurtén^{*,†}
23
24
25
26

27 *Department of Chemistry and Institute for Atmospheric and Earth System Research (INAR),*
28 *University of Helsinki, P.O. Box 55, FI-00014, Helsinki, Finland, Department of Chemistry,*
29 *University of Helsinki, P.O. Box 55, FI-00014, Helsinki, Finland, Department of Chemistry,*
30 *University of Helsinki, P.O. Box 55, FI-00014, Helsinki, Finland, Department of Chemistry,*
31 *University of Copenhagen, DK-2100 Copenhagen Ø, Denmark, and Department of Physics*
32 *and Institute for Atmospheric and Earth System Research (INAR), University of Helsinki,*
33 *P.O. Box 64, FI-00014, Helsinki, Finland*
34
35
36
37
38
39

40 E-mail: siddharth.iyer@helsinki.fi; theo.kurten@helsinki.fi
41
42
43
44

45 **Abstract**

46
47 The oxidation of biogenically emitted volatile organic compounds (BVOC) plays an
48 important role in the formation of secondary organic aerosols (SOA) in the atmosphere.
49
50 Peroxy radicals (RO₂) are central intermediates in the BVOC oxidation process. Under
51

52 *To whom correspondence should be addressed

53 †University of Helsinki

54 ‡University of Helsinki

55 ¶University of Copenhagen

56 §University of Helsinki
57
58
59
60

clean (low- NO_x) conditions, the main bimolecular sink reactions for RO_2 are with the hydroperoxy radical (HO_2) and with other RO_2 radicals. Especially for small RO_2 , the $\text{RO}_2 + \text{HO}_2$ reaction mainly leads to closed-shell hydroperoxide products. However, there exist other known $\text{RO}_2 + \text{HO}_2$ and $\text{RO}_2 + \text{RO}_2$ reaction channels that can recycle radicals and oxidants in the atmosphere, potentially leading to lower-volatility products and enhancing SOA formation. In this work, we present a thermodynamic overview of two such reactions: **a)** $\text{RO}_2 + \text{HO}_2 \rightarrow \text{RO} + \text{OH} + \text{O}_2$ and **b)** $\text{R}'\text{O}_2 + \text{RO}_2 \rightarrow \text{R}'\text{O} + \text{RO} + \text{O}_2$ for selected monoterpene + oxidant derived peroxy radicals. The monoterpenes considered are α -pinene, β -pinene, limonene, trans- β -ocimene, and Δ^3 -carene. The oxidants considered are the hydroxyl radical (OH), the nitrate radical (NO_3), and ozone (O_3). The reaction Gibbs energies were calculated at the DLPNO-CCSD(T)/def2-QZVPP// ω B97X-D/aug-cc-pVTZ level of theory. All reactions studied here were found to be exergonic in terms of Gibbs energy. Based on a comparison with previous mechanistic studies, we predict that reaction **a** and reaction **b** are likely most important for first-generation peroxy radicals from O_3 oxidation (especially for β -pinene), while less so for most first-generation peroxy radicals from OH and NO_3 oxidation. This is because both reactions are comparatively more exergonic for the O_3 oxidized systems than their OH and NO_3 oxidized counterparts. Our results indicate that bimolecular reactions of certain complex RO_2 may contribute to an increase in radical and oxidant recycling under high HO_2 conditions in the atmosphere, which can potentially enhance SOA formation.

Introduction

Biogenically emitted volatile organic compounds (BVOCs) play a critical role in the formation and growth of atmospheric secondary organic aerosol particles (SOA).¹⁻⁴ Once they have grown to sufficient sizes (on the order of ~ 100 nm), aerosol particles can affect the Earth's climate both directly, by reflecting solar radiation, and indirectly, by serving as cloud condensation nuclei, and thus modifying cloud properties such as reflectivity and lifetime.⁵

1
2
3
4
5 33 Isoprene (C₅H₈) and monoterpenes, a class of VOCs with the chemical formula C₁₀H₁₆,
6
7 34 are the most abundant BVOC emissions, accounting for about 69% and 11% of the total
8
9 35 global BVOC emission, respectively.⁶ These molecules undergo gas-phase reactions with the
10
11 36 atmospheric oxidants such as the hydroxyl radical (OH), the nitrate radical (NO₃) and ozone
12
13 37 (O₃), forming peroxy radicals (RO₂). Unimolecular reaction pathways of peroxy radicals have
14
15 38 recently been demonstrated to be important, especially for the formation of highly oxidized
16
17 39 multifunctional organic compounds (HOM) through the process of autoxidation.^{4,7} HOMs
18
19 40 can have very low volatilities, allowing them to condense and form particles very effectively.
20
21 41 Other peroxy radical reaction pathways generally lead to less oxidized and more volatile
22
23 42 products, which may nevertheless also contribute to the growth of particulate matter.

24
25 43
26
27 44 α -pinene, β -pinene, limonene, trans- β -ocimene, and Δ^3 -carene together account for close
28
29 45 to 90% of the global monoterpene emissions.⁶ The reaction of monoterpenes with the at-
30
31 46 mospheric oxidants initiates the process that leads to the formation of a range of products,
32
33 47 including the multi-functionalized HOMs. OH initiated oxidation of alkenes can involve either
34
35 48 OH radical addition to one of the olefinic carbon atoms, or the abstraction of an aliphatic
36
37 49 hydrogen atom. In both cases, the product is an alkyl radical. O₂ can rapidly add to alkyl
38
39 50 radicals to form a peroxy radical RO₂.⁸ For simple alkyl radicals, a pseudo-unimolecular
40
41 51 rate of $\sim 10^7 \text{s}^{-1}$ is often assumed for the O₂ + alkyl reaction when the O₂ partial pressure is
42
43 52 approximately 0.2 atm.^{9,10} NO₃ oxidation also involves addition to one of the olefinic carbon
44
45 53 atoms of the alkene (though, in some cases, hydrogen atom abstraction may compete^{11,12}),
46
47 54 followed by the O₂ addition to the subsequent alkyl radical to form the RO₂. The RO₂
48
49 55 contains an ONO₂ functionality, and closed-shell reaction products retaining this group are
50
51 56 commonly called organonitrates. Organonitrates are important in the atmosphere as they
52
53 57 can serve as a NO_x (where, x=1,2) reservoir.¹³ Ambient measurements have discovered that
54
55 58 organonitrates make up a significant fraction of SOA.^{14,15}

1
2
3
4
59

5 Ozone oxidation produces peroxy radicals that are structurally different from the peroxy
6 radicals formed following OH or NO₃ oxidation. There are multiple known channels for
7
8
9
10
11
12
13
14
15
16
17
18
19
20
21
22
23
24
25
26
27
28
29
30
31
32
33
34
35
36
37
38
39
40
41
42
43
44
45
46
47
48
49
50
51
52
53
54
55
56
57
58
59
60

60 Ozone oxidation produces peroxy radicals that are structurally different from the peroxy
61 radicals formed following OH or NO₃ oxidation. There are multiple known channels for
62 alkene + ozone reactions. For RO₂ formation, the main channel involves the formation and
63 subsequent decomposition of a vinylhydroperoxide (VHP). Ozonolysis of alkenes (see Figure 2)
64 is initiated by addition of O₃ across the double bond, forming a primary ozonide (POZ). The
65 POZ then rapidly decomposes, forming a Criegee intermediate (CI; a carbonyl oxide) and a
66 carbonyl group. In the case of endocyclic alkenes, such as α -pinene, limonene, and Δ^3 -carene,
67 the CI and carbonyl groups remain within the same molecule. For exocyclic, or acyclic
68 alkenes, such as β -pinene and trans- β -ocimene, POZ decomposition leads to fragmentation of
69 the molecule. In the VHP channel, the CI forms a VHP following a 1,4 hydrogen shift (VHP
70 formation may or may not be preceded by collisional stabilization of the CI¹⁶). The VHP
71 quickly loses an OH, forming a vinoxy radical, which adds O₂ to form the first-generation RO₂.

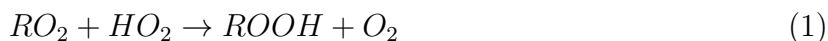
72

73 Monoterpenes (and other alkene VOCs) are thus eventually converted to peroxy radicals
74 by all the main atmospheric oxidants. A myriad of possible unimolecular and bimolecular
75 reactions in the atmosphere determine the fate of these radicals. The chemistry of simpler
76 RO₂ has been explored in detail previously (Orlando et al. 2012¹⁷ and references therein).
77 Over regions with significant anthropogenic emissions, NO can react with RO₂ to produce
78 alkoxy radicals (organonitrate formation is a competing, but generally minor, channel).¹⁷ This
79 is a radical propagating channel, leading also to NO₂, which contributes to the formation of
80 O₃ and ultimately OH (and HO₂).¹⁸ In more pristine conditions that are relatively unaffected
81 by anthropogenic emissions, RO₂ are more likely to react with HO₂ or other RO₂, or undergo
82 unimolecular reactions.

83

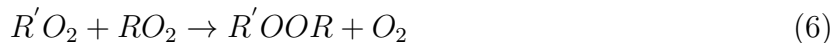
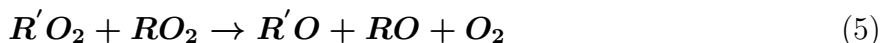
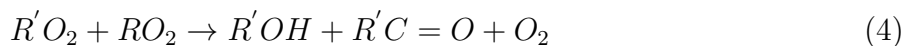
84 The RO₂ + HO₂ channel becomes relevant in low NO_x conditions, where the lifetime
85 of RO₂ is long enough to react with the HO₂ radical. The RO₂ + HO₂ reaction is usually

1
2
3
4 86 assumed to be a radical sink process, forming (mostly) stable hydroperoxides¹⁹ (reaction
5
6 87 1). However, other known $RO_2 + HO_2$ reaction channels (reaction 2 and reaction 3) can
7
8 88 potentially be important and result in radical and oxidant recycling in the atmosphere:
9



13
14
15
16
17
18
19
20 91 Reaction 2 leads to the formation of alkoxy radicals. These radicals can continue oxidation in
21
22 92 the atmosphere^{20,21} and may lead to products with lower volatilities than the ROOH product
23
24 93 of reaction 1. Since the reaction also serves to recycle OH, it can enhance VOC oxidation.
25
26 94 Studies of the branching ratios of the two reactions have only been performed for relatively
27
28 95 small hydrocarbons (up to 3 carbon atoms).^{19,22,23}
29

30
31
32 97 The $RO_2 + RO_2$ reaction has three known channels:
33
34



38
39
40
41
42
43
44
45 100 Reactions 4 and 6 are both radical termination reactions. Reaction 6 is generally unimportant
46
47 101 for small RO_2 , but it has been suggested as a mechanism for the lowest-volatility "dimer"
48
49 102 reaction products observed in experiments on e.g. monoterpenes.^{1,24} Reaction 5 is a radical
50
51 103 propagation reaction, and leads to reactive alkoxy radicals analogously to reaction 2. The
52
53 104 branching between the competing reaction pathways for both $RO_2 + HO_2$ and $RO_2 + RO_2$
54
55 105 reactions are thus important for the radical recycling of the atmosphere.
56
57
58
59
60

106

1
2
3
4
5 107 In this work, we carry out a thermodynamic study of the favorability of the radical-recycling
6
7 108 reactions 2 and 5 for a set of the most common monoterpenes and oxidants in the atmosphere.
8
9 109 Only the first generation RO₂ is considered, i.e., the RO₂ formed by the first O₂ addition
10
11 110 to the alkyl radical following oxidation. Despite this restriction, our study encompasses
12
13 111 83 different RO₂ species, and a total of 3486 possible reactions for reaction 5. We also
14
15 112 compute thermodynamic parameters for reaction 3, which has previously been observed for
16
17 113 carbonyl-containing acyl peroxy radicals.^{19,22,23} It is unlikely that any of the non-acyl peroxy
18
19 114 radicals studied here will undergo direct bimolecular reactions with HO₂ to form O₃, as
20
21 115 no mechanism has been identified for this in the literature. However, the reaction might
22
23 116 conceivably occur in the presence of catalysts, either in the gas-phase via clustering, or in
24
25 117 the atmospheric condensed phase. The reaction Gibbs energies for this reaction are provided
26
27 118 in Table S1 in the SI. The transition states and associated rates of reactions for the oxidized
28
29 119 monoterpenes were not studied in this work because of the large set of reactions and the size
30
31 120 of the individual reactants and products considered here.

121 **Methods**

122 The computational methods employed here have been described in detail previously.^{8,25,26} The
123
124 123 systems studied here possess multiple different isomers, each with a large number of potential
125
126 124 conformers. In this context, isomers are defined as compounds with the same chemical
127
128 125 elemental composition (and in this case also the same functional groups), but differing in
129
130 126 their bonding patterns (i.e. positional isomers). Interconversion of different isomers typically
131
132 127 involves the breaking of covalent bonds, and is thus associated with high barriers. Conformers,
133
134 128 on the other hand, have identical bonding patterns, and differ only in the three-dimensional
135
136 129 arrangement of atoms. Conformers can be interconverted by rotations around torsional angles,
137
138 130 which typically have low energy barriers in comparison to reactions breaking and forming

1
2
3 131 bonds.
4
5
6 132

7 133 The conformer sampling for each isomer was carried out by a systematic conformer search using
8
9 134 the MMFF force field,²⁷⁻³² followed by single-point energy calculations and geometry optimiza-
10
11 135 tions at the B3LYP/6-31+G(d) level of theory.³³⁻³⁸ Spartan '14 and '16 were used to carry
12
13 136 out these computations.^{39,40} For the RO₂s and the ROs, the keyword "FFHINT=O_x ~6"
14
15 137 (*x*=radical oxygen atom number as labeled by the Spartan program) was used to denote
16
17 138 the radical oxygen and to specify its atom type to "generic divalent O", which was found to
18
19 139 yield good results for peroxy radicals.^{38,41} Following initial single-point calculations on all
20
21 140 the conformers, those within 5 kcal/mol in relative electronic energies of the lowest-energy
22
23 141 conformer were optimized at the B3LYP/6-31+G(d) level. Conformers within 2 kcal/mol
24
25 142 in relative electronic energy following the optimization were then optimized at the ωB97X-
26
27 143 D/aug-cc-pVTZ⁴²⁻⁴⁴ level using the Gaussian 09 program.⁴⁵ The calculations were performed
28
29 144 using an ultrafine integration grid. Since there were multiple conformers for every reactant
30
31 145 and product isomer, the reaction energies were calculated using conformationally averaged
32
33 146 Gibbs energies. The equation for calculating the conformationally averaged Gibbs energy, *G*,
34
35 147 is:⁴⁶

$$G = -k_B T \ln \left(e^{-\beta g_0} \sum_k e^{-\beta (g_k - g_0)} \right), \quad (7)$$

36
37
38
39
40 148 where, *g*₀ is the Gibbs energy of the most energetically favorable conformer, $\beta = 1/k_B T$, *g*_{*k*}
41
42 149 is the Gibbs energy of the *k*th conformer relative to *g*₀, *k*_B is the Boltzmann constant, and *T*
43
44 150 is the temperature. The Gibbs energies for each individual conformer was computed using
45
46 151 the standard rigid rotor and harmonic oscillator approximations, with the temperature set to
47
48 152 298.15 K and with a reference pressure of 1 atm (values at different conditions can be com-
49
50 153 puted using the log files provided in a supplementary information file). The conformationally
51
52 154 averaged Gibbs energies were then corrected using DLPNO-CCSD(T)/def2-QZVPP single
53
54 155 point energies calculated using the ORCA program.^{47,48} The DLPNO-CCSD(T)/def2-QZVPP
55
56 156 single point calculation was performed on the lowest energy conformer geometry and the
57
58
59
60

1
2
3
4 157 conformationally averaged Gibbs energy was corrected by the difference between the DFT
5
6 158 and DLPNO-CCSD(T) electronic energies of the lowest energy conformer. DLPNO stands
7
8 159 for domain-based local pair natural orbitals. Instead of canonical delocalized orbitals, the
9
10 160 method uses pair natural orbitals that are then localized and classified into domains for
11
12 161 sorting and selection of the most important excitations that account for electronic correlation.
13
14 162 The DLPNO-CCSD(T) method also differs from corresponding canonical methods when
15
16 163 evaluating the triples, using the T_0 approximation which neglects the elements outside the
17
18 164 diagonal in the Fock Matrix. This greatly reduces the calculation time. The accuracy of the
19
20 165 DLPNO-CCSD(T) method has been tested previously by comparing the DLPNO-CCSD(T)
21
22 166 calculated formation enthalpies with accurate formation enthalpies for a set of 113 molecules
23
24 167 and found to have a mean absolute error of 1.6 kcal/mol.⁴⁹

25
26 168
27 169 Test calculation were performed on small systems with the same functionalities as the
28
29 170 molecules studied here to determine the transition state energies for the reaction $RO_2 + HO_2$
30
31 171 $\rightarrow RO + OH + O_2$ (reaction 2). The transition states were calculated for $CH_2(OH)CH_2OO$
32
33 172 and $CH_2(ONO_2)CH_2OO$ systems (analogous to those formed from OH and NO_3 oxidation) at
34
35 173 the CBS/QB3 level,⁵⁰ which was used by Hasson et al.²³ for similar systems. These transition
36
37 174 states are open-shell singlets and were therefore calculated using unrestricted UCBS-QB3 with
38
39 175 the Guess=(mix,always) keyword. This mixes the HOMO and the LUMO so as to destroy
40
41 176 the α and β spatial symmetries and requests a new initial guess to be generated at each point
42
43 177 in the optimization. The spin contamination in the UHF steps in the CCSD(T) and MP2
44
45 178 calculations in UCBS-QB3 were ~ 1.05 before and ~ 0.9 after annihilation. The energetics
46
47 179 of the intermediate complex of reaction $RO'_2 + RO_2 \rightarrow R'O + RO + O_2$ (reaction 5) was
48
49 180 studied by optimizing $CH_3CH_2O \cdots O_2 \cdots OCH_2CH_3$ at the M11/6-31+G(d,p)^{35,51-53} level
50
51 181 of theory employed in Lee et al.⁵⁴

52
53 182
54
55 183 The reaction Gibbs energies for reactions 2, 3 and 5 were calculated by subtracting the
56
57
58
59
60

1
2
3
4
5
6
7
8
9
10
11
12
13
14
15
16
17
18
19
20
21
22
23
24
25
26
27
28
29
30
31
32
33
34
35
36
37
38
39
40
41
42
43
44
45
46
47
48
49
50
51
52
53
54
55
56
57
58
59
60

184 Gibbs energies of the free products from the Gibbs energies of the free reactants:

$$\Delta G(\text{Reaction 2}) = [G(\text{RO}) + G(\text{OH}) + G(\text{O}_2)] - [G(\text{RO}_2) + G(\text{HO}_2)] \quad (8)$$

$$\Delta G(\text{Reaction 3}) = [G(\text{ROH}) + G(\text{O}_3)] - [G(\text{RO}_2) + G(\text{HO}_2)] \quad (9)$$

$$\Delta G(\text{Reaction 5}) = [G(\text{R}'\text{O}) + G(\text{RO}) + G(\text{O}_2)] - [G(\text{R}'\text{O}_2) + G(\text{RO}_2)] \quad (10)$$

187 The structures of the monoterpenes studied here are shown in Figure 1. For α -pinene and
188 β -pinene, the "-" enantiomers were considered, while for limonene and Δ^3 -carene the "+"
189 enantiomers were considered. As the other enantiomers are mirror images, their energetics
190 are identical. For ocimene, trans- β -ocimene was studied as it makes up the majority of the
191 biogenic ocimene emission.⁶

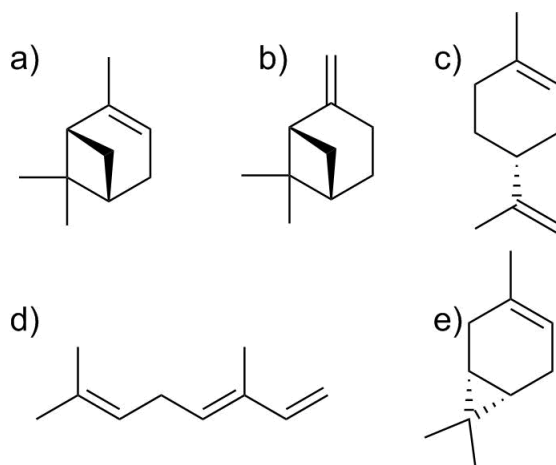


Figure 1: Monoterpene isomers investigated in this study. a) α -pinene, b) β -pinene, c) limonene, d) trans- β -ocimene, and e) Δ^3 -carene.

192 Depending on which olefinic carbon is attacked by the oxidants, multiple isomers of
193 the first-generation RO_2 are possible. For RO_2 s from OH and NO_3 oxidation, we generally
194 consider only those isomers formed by addition to the double bond where the initial alkyl
195 radical is formed on the most substituted (tertiary) carbon atom. However, for β -pinene,
196 which has a very limited number of RO_2 isomers from OH and NO_3 oxidation, all first-

1
2
3 197 generation isomers were calculated to see the effect on the reaction energy. All possible
4
5 198 first-generation isomers were also calculated for trans- β -ocimene, including resonance isomers
6
7 199 from ozone oxidation. Oxidation via H-abstraction by OH is possible (and can account
8
9 200 for a significant fraction of OH oxidation products of monoterpenes according to Rio et al.
10
11 201 2010⁵⁵). However, we decided to limit our study to only oxidation via OH addition as, accord-
12
13 202 ing to current knowledge, it is still the dominant OH oxidation pathway for monoterpenes.^{55,56}
14
15 203
16
17 204 For the ozonolysis reaction, the RO₂ radicals with more than one carbon atom formed
18
19 205 via the VHP pathway were considered. The mechanism for trans- β -ocimene is illustrated in
20
21 206 Figure 2. For limonene, we only consider ozone attack on the endocyclic double bond, as it
22
23 207 has been reported to be 35 times more favorable than the attack on the exocyclic double
24
25 208 bond.⁵⁷ β -pinene is an exocyclic alkene and thus does not undergo a ring-opening reaction, but
26
27 209 instead loses the CH₂ group in the form of formaldehyde (CH₂O) in the POZ decomposition.
28
29 210 The CI formed by ozone attack on the terminal double bond of trans- β -ocimene can not form
30
31 211 a VHP (as there is no H atom to abstract in a 1,4 H-shift), and this reaction site was thus
32
33 212 omitted from our study. Since ozonolysis leads to the breaking of a C=C bond, the RO₂
34
35 213 products of limonene ozonolysis are acyclic, while those of α -pinene and Δ^3 -carene have lost
36
37 214 their 6-membered rings, but retain their 4- and 3-membered rings, respectively.
38
39
40
41
42
43
44
45
46
47
48
49
50
51
52
53
54
55
56
57
58
59
60

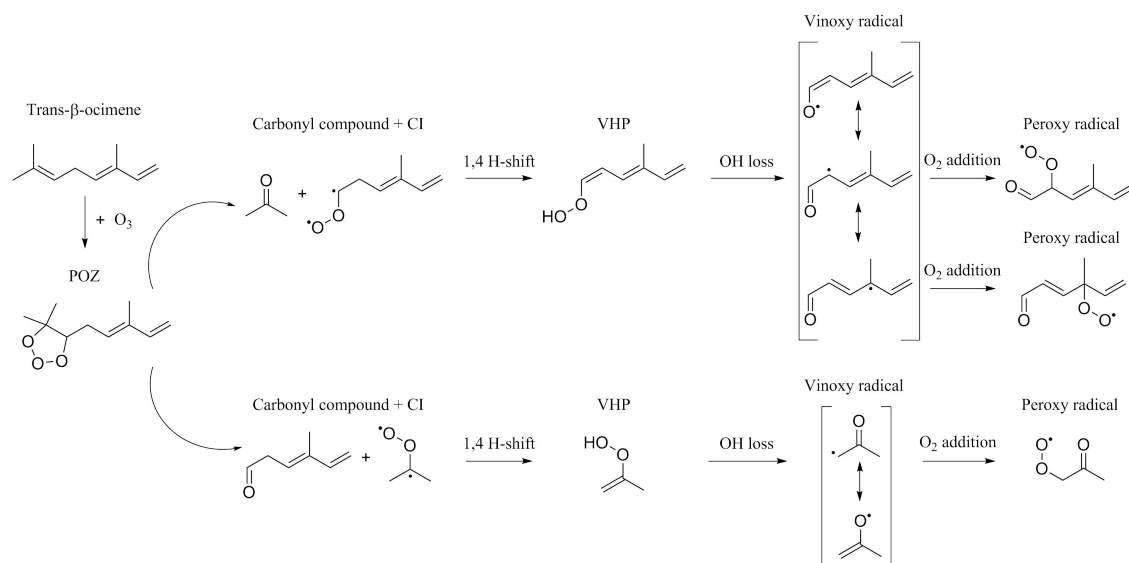


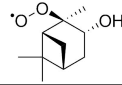
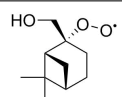
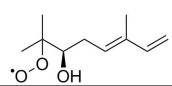
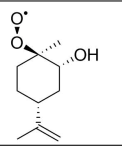
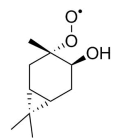
Figure 2: Ozonolysis reaction of trans-β-ocimene over one of the double bonds. The primary ozonide (POZ) can decompose via two possible Criegee intermediate (CI) and carbonyl compound forming channels. The CI forms a vinyl hydroperoxide (VHP) by a 1,4 hydrogen shift, followed by OH loss to form a vinoxy radical. The vinoxy radical then adds an oxygen molecule, forming a peroxy radical.

Results

RO₂ + HO₂ reaction for RO₂ radicals from OH and NO₃ oxidation

The general mechanisms for the initial steps of oxidation via OH and NO₃ addition to double bonds are identical, and the results for the HO₂ reactions with OH and NO₃-derived RO₂ radicals are therefore presented in the same section. The schematic of the lowest energy RO₂ radical isomer is shown in Table 1 for the OH oxidized case and in Table 2 for the NO₃ oxidized case, with the range (maximum-minimum) of Gibbs energies given for the full set of isomers. All reaction Gibbs energies are provided in Tables S4-S8 in the SI. The log files needed to compute them are also provided in the supplementary zip archive.

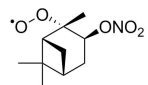
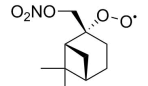
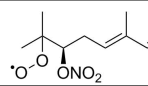
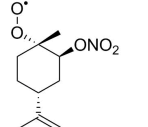
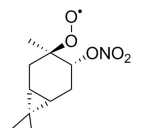
Table 1: Range of Reaction Gibbs Energies (ΔG) in kcal/mol for Different Isomers For the OH Oxidized Monoterpenes in the $\text{RO}_2 + \text{HO}_2 \rightarrow \text{RO} + \text{OH} + \text{O}_2$ Reaction

Monoterpene	Isomer ^a	ΔG^b
α -pinene		-0.12 to -6.40
β -pinene		-2.03 to -4.88
Trans- β -ocimene		-1.47 to -3.85
Limonene		-1.11 to -2.61
Δ^3 -carene		-1.34 to -4.70

^a Lowest energy RO_2 isomer (in terms of Gibbs energy at 298.15 K).

^b Gibbs energies (at 298.15 K and 1 atm reference pressure) are conformationally averaged and calculated at the DLPNO-CCSD(T)/def2-QZVPP// ω B97X-D/aug-cc-pVTZ level.

Table 2: Range of Reaction Gibbs Energies (ΔG) in kcal/mol for Different Isomers For the NO_3 Oxidized Monoterpenes in the $\text{RO}_2 + \text{HO}_2 \rightarrow \text{RO} + \text{OH} + \text{O}_2$ Reaction

Monoterpene	Isomer ^a	ΔG^b
α -pinene		-1.79 to -5.25
β -pinene		-1.74 to -4.88
Trans- β -ocimene		-1.78 to -5.52
Limonene		-1.63 to -4.40
Δ^3 -carene		-2.13 to -5.75

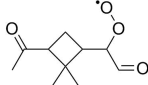
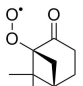
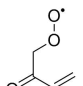
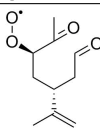
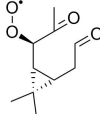
^a Lowest energy RO_2 isomer (in terms of Gibbs energy at 298.15 K).

^b Gibbs energies (at 298.15 K and 1 atm reference pressure) are conformationally averaged and calculated at the DLPNO-CCSD(T)/def2-QZVPP// ω B97X-D/aug-cc-pVTZ level.

224 $\text{RO}_2 + \text{HO}_2$ reaction for RO_2 from ozonolysis

225 The range (maximum-minimum) of the reaction Gibbs energies for the different isomers of
 226 the ozonolysis derived RO_2 s are given in Table 3, with the schematic of the lowest energy
 227 RO_2 also shown. The ozonolysis of trans- β -ocimene leads to the formation of peroxy radicals
 228 with different elemental compositions which are not isomers of each other. Therefore, the
 229 reaction energies for each of the different trans- β -ocimene derived RO_2 s are shown separately
 230 in Table 4.

Table 3: Range of Reaction Gibbs Energies (ΔG) in kcal/mol For Different Isomers for the O_3 Oxidized Monoterpenes in the $RO_2 + HO_2 \rightarrow RO + OH + O_2$ Reaction

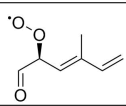
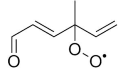
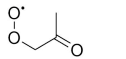
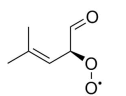
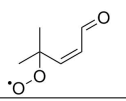
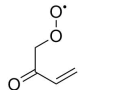
Monoterpene	Isomer ^a	ΔG^b
α -pinene		-4.03 to -4.16 (-26.64,-25.42) ^c
β -pinene		-4.24 to -7.16
Trans- β -ocimene		-2.38 to -4.68
Limonene		-4.02 to -4.70
Δ^3 -carene		-2.09 to -4.70

^a Lowest energy RO_2 isomer (in terms of Gibbs energy at 298.15 K).

^b Gibbs energies (at 298.15 K and 1 atm reference pressure) are conformationally averaged and calculated at the DLPNO-CCSD(T)/def2-QZVPP// ω B97X-D/aug-cc-pVTZ level.

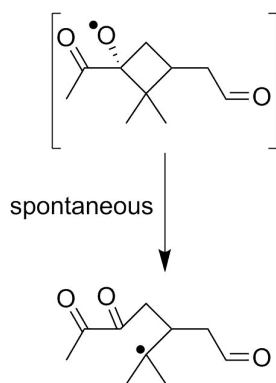
^c Includes alkoxy ring-breaking step as no alkoxy radical minimum could be found.

Table 4: Reaction Gibbs Energies (ΔG) in kcal/mol for All The Trans- β -Ocimene Ozonolysis Isomers Considered In This Study in the $\text{RO}_2 + \text{HO}_2 \rightarrow \text{RO} + \text{OH} + \text{O}_2$ Reaction

RO ₂	Isomer	ΔG^a
1		-2.70
2		-2.37
3		-4.03
4		-2.37
5		-1.97
6		-4.68

^a Gibbs energies (at 298.15 K and 1 atm reference pressure) are conformationally averaged and calculated at the DLPNO-CCSD(T)/def2-QZVPP// ω B97X-D/aug-cc-pVTZ level.

The RO₂s from α -pinene ozonolysis with the radical group located on the ring were excluded from the study due to a previously reported ring-breaking reaction that occurs spontaneously upon formation of the RO product,⁸ making the alkoxy forming channel significantly exergonic. In this reaction, the alkoxy oxygen forms a carbonyl group, breaking the four-member cyclobutyl ring in the process, forming a second-generation alkyl radical, as shown in Figure 3. Reaction thermodynamics for the other two RO₂s formed in α -pinene ozonolysis are comparable to the other monoterpenes.

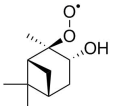
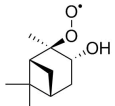
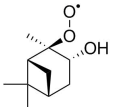
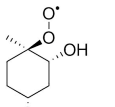
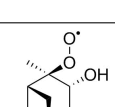
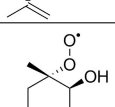
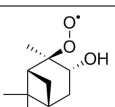
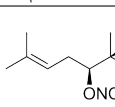
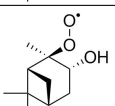
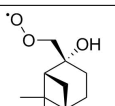
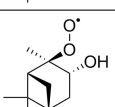
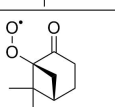
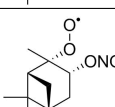
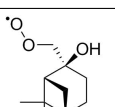
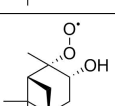
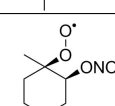
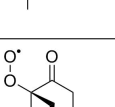
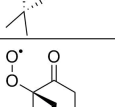


17 Figure 3: Ring breaking reaction observed during the optimization of the RO product for the
18 most favorable RO₂ isomer product following ozonolysis of α-pinene.
19
20
21

22 **R'O₂ + RO₂ → R'O + RO + O₂ reaction**
23

24
25 239 For reaction 5, 83 self-reactions + (83×82)/2 cross-reactions were possible, giving a total
26
27 240 of 3486 reactions when all the monoterpene + oxidant combinations were considered. The
28
29 241 reaction Gibbs energies varied from a maximum of -2.86 kcal/mol to a minimum of -16.96
30
31 242 kcal/mol. Table 5 shows the reaction Gibbs energies of a select few reactions categorized
32
33 243 into reaction energy ranges of 0 to -5, -5 to -10, and -10 to -17 kcal/mol. Reaction Gibbs
34
35 244 energy ranges were used to point out important RO₂/RO features that were found to strongly
36
37 245 influence the reaction Gibbs energies. The complete set of reaction Gibbs energies is provided
38
39 246 as an Excel spreadsheet in the supplementary material.
40
41
42
43
44
45
46
47
48
49
50
51
52
53
54
55
56
57
58
59
60

Table 5: Reaction Gibbs Energies (ΔG) in kcal/mol for Selected $R'O_2 + RO_2 \rightarrow R'O + RO + O_2$ Reactions

Range	Isomer		ΔG^a	
	$R'O_2$	RO_2		
0 to -5	a			-2.86
	b			-3.86
	c			-4.08
-5 to -10	d			-5.90
	e			-7.63
	f			-9.91
-10 to -17	g			-12.40
	h			-14.78
	i			-16.96

^a Gibbs energies (at 298.15 K and 1 atm reference pressure) are conformationally averaged and calculated at the DLPNO-CCSD(T)/def2-QZVPP// ω B97X-D/aug-cc-pVTZ level.

247 The reaction Gibbs energies of reaction 5 point to low favorability for the reactions
 248 involving the OH-oxidized α -pinene isomer with the RO_2 functional group and OH functional
 249 group on the opposite sides of the ring. The first six entries in Table 5 all have this isomer as

1
2
3 250 the R'O₂ reactant to help illustrate how the identity of the other peroxy radical changes the
4
5 251 reaction thermodynamics.
6
7
8

9 252 **Discussion and Atmospheric Implications**

10
11
12 253 All reactions studied here had standard Gibbs energies below 0. However, while important,
13
14 254 this is not a sufficient condition for a reaction to be competitive under atmospheric conditions.
15
16 255 The atmospheric importance of a reaction depends on its reaction rate. While reaction rates
17
18 256 cannot be determined from the thermodynamic parameters reported here, some general
19
20 257 guidelines can help illustrate which reactions might be competitive in atmospheric conditions,
21
22 258 and which can be ruled out.
23
24

25 259
26
27 260 Most of the reactions studied here likely involve transition states, or at least reactant
28
29 261 complexes or reaction intermediates, which suffer from an entropy penalty compared to the
30
31 262 free reactants (or products) due to the loss of translational and rotational degrees of freedom.
32
33 263 This is especially important for reaction 2 and reaction 5, where two reactants first combine,
34
35 264 and then separate to form three products, with an associated gain in entropy. Our discussion
36
37 265 here focuses on parameters computed at 298.15 K. The rates of bimolecular radical reactions
38
39 266 in the atmosphere are typically not very temperature-sensitive (as the enthalpy barriers of
40
41 267 competitive reaction channels are inevitably fairly close to zero), and the general conclusions
42
43 268 drawn here can thus likely be applied to most of the lower troposphere. Thermodynamic
44
45 269 parameters at other temperatures can be computed from the data in the log files (provided
46
47 270 as a supplementary material zip archive).
48
49



52
53 272 The overall entropy gain in reaction 2 translates to a difference of around 9-10 kcal/mol
54
55 273 between the reaction enthalpies and the reaction Gibbs energies (computed at the ωB97X-
56
57
58
59
60

1
2
3
4 274 D/aug-cc-pVTZ level as the thermal contributions to the Gibbs energy are available only at
5
6 275 this level). Similarly, the entropy contributions to the Gibbs energies ($-T\Delta S$) of the transition
7
8 276 states and/or intermediates for reaction 2 must be around 20 kcal/mol higher than those of
9
10 277 the products. If the transition states and products were isoenergetic in terms of the enthalpy,
11
12 278 a reaction Gibbs energy of 0 kcal/mol would thus imply a barrier of about 20 kcal/mol –
13
14 279 making the reaction much too slow to matter in the atmosphere.

280

17 281 In reality, the transition states and separated products are not isoenergetic – either can
18
19 282 contain both stabilizing and destabilizing interactions that are lacking in the other. Hasson
20
21 283 et al.²³ found that for ethyl peroxy and acetyl peroxy radicals, the rate-limiting transition
22
23 284 states for reaction 2 were 7.5 and 13.7 kcal/mol below the separated products in enthalpies,
24
25 285 respectively (the transition states can be lower than the products due to the presence of
26
27 286 multiple intermediates or product complexes on the reaction path).

287

31 288 The entropy contribution to the Gibbs energy of the transition state relative to the products,
32
33 289 and the stabilization of the transition state due to inter-molecular interactions, were further
34
35 290 investigated for reaction 2 by performing test calculations on small systems with the same
36
37 291 functionalities as the OH and NO₃ oxidized RO₂ (two-carbon systems CH₂(OH)CH₂OO
38
39 292 and CH₂(ONO₂)CH₂OO). The analogous system for O₃ oxidation is the acetyl peroxy
40
41 293 radical, which was already studied by Hasson et al.²³ The enthalpies, entropy contributions
42
43 294 ($-T\Delta S$), and Gibbs energies for key stationary points of the CH₂(OH)CH₂OO + HO₂ →
44
45 295 CH₂(OH)CH₂O + OH + O₂ reaction are shown in Figure 4. Only the rate limiting transi-
46
47 296 tion state energy is shown. There are multiple intermediates and transition states between
48
49 297 intermediate 2 (INT₂ in Figure 4) and the separated products. Hasson et al.²³ provide the
50
51 298 entire reaction pathway for alkyl, acyl, and acetyl type RO₂s. The transition states for the
52
53 299 OH- and NO₃-oxidized systems were found to be 12.4 kcal/mol and 13.2 kcal/mol lower in
54
55 300 enthalpies, respectively, than the corresponding free products (these values were calculated

at the same computational level employed in Hasson et al.- CBS-QB3²³). This is very similar to the value of 13.7 kcal/mol found for the acetyl peroxy radical, indicating that transition states for all RO₂ + HO₂ reactions studied here are stabilized (in enthalpy, compared to the free products) by roughly similar amounts. The entropy contribution to the Gibbs energy of the transition state relative to the free products was 21.5 and 21.8 kcal/mol for OH- and NO₃-oxidized systems, respectively (and 23.6 kcal/mol for the acetyl peroxy radical²³). In terms of Gibbs energy (accounting for both the entropy contribution to the transition state Gibbs energy and the stabilization of the transition state due to favorable intra-molecular interactions) the transition states were thus 9.4, 8.0, and 9.9 kcal/mol above the reactants for the OH-, NO₃, and O₃ oxidized systems, respectively.

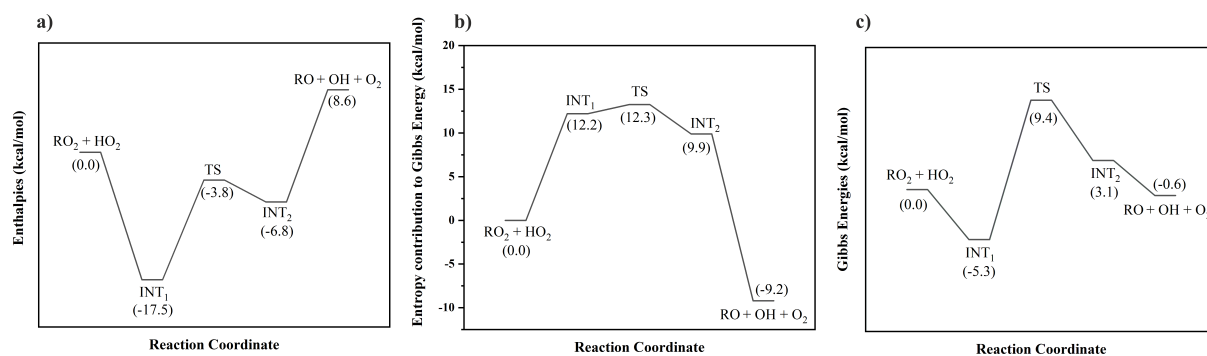


Figure 4: Reaction stationary points for the RO₂ + HO₂ reaction, where the RO₂ = CH₂(OH)CH₂OO, in terms of a) enthalpies and c) Gibbs energies. b) shows the entropy contribution ($-T\Delta S$ at 298.15 K) to the Gibbs energies calculated at the CBS-QB3 level of theory. INT = intermediate, TS = transition state.

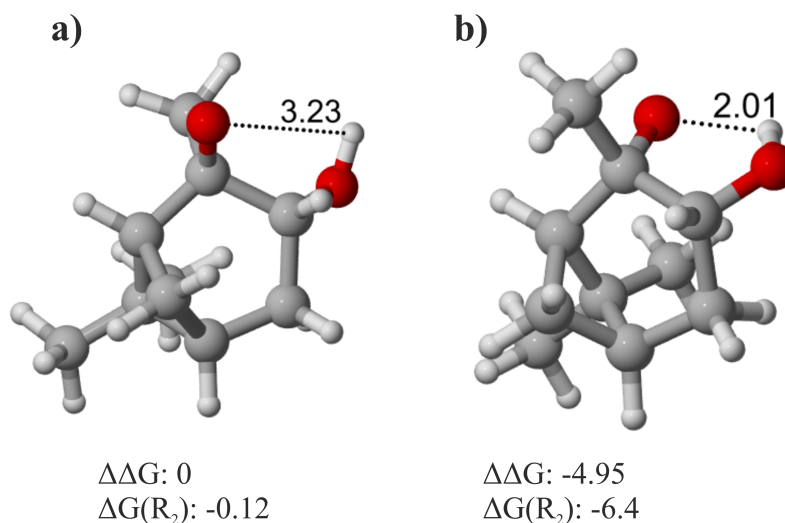
The overall rates (including all channels) for RO₂ + HO₂ reactions are typically on the order of 10^{-11} cm³ molecules⁻¹ s⁻¹, and they typically increase with the size of the RO₂.⁵⁸ For a particular reaction channel (such as reaction 2) to be competitive, its rate can thus not be much lower than this. Using elementary transition state theory, a rate of 10^{-11} cm³ molecules⁻¹ s⁻¹ corresponds to a Gibbs energy barrier of approximately 5 kcal/mol. Based on our test calculations and Hasson et al.,²³ for the two-carbon systems, the entropy penalty to the Gibbs energy of the transition states is about 22 kcal/mol relative to the products, while

1
2
3 318 the TS enthalpies are about 13 kcal/mol below the products of reaction 2 due to favorable
4
5 319 intra-molecular interactions. Thus, for the Gibbs energy barrier to be 5 kcal/mol or less, the
6
7 320 Gibbs energy of reaction 2 should not be higher than -4 kcal/mol. While our test systems
8
9 321 have the same functional groups as the molecules in this study, the calculated $-T\Delta S$ and
10
11 322 enthalpic contributions to the transition state Gibbs energy of reaction 2 cannot be assumed
12
13 323 to be directly applicable to all the monoterpene derived reactants and products studied here.
14
15 324 However, test calculations on one α -pinene derived RO_2 (see section S3 in the SI) indicate
16
17 325 that our "rule of thumb" may be reasonably valid also for larger systems, and can thus be
18
19 326 helpful in gauging what reactions are likely to be competitive. We can conclude therefore
20
21 327 that any example of reaction 2 with an overall Gibbs energy much above -4 kcal/mol is
22
23 328 unlikely to be competitive in the atmosphere. As seen from tables 1 to 4, this includes most
24
25 329 (though not all) of the OH and NO_3 derived 1st generation RO_2 , and some of the RO_2 from
26
27 330 O_3 oxidation of trans- β -ocimene and Δ^3 -carene. On the other hand, for each monoterpene +
28
29 331 oxidant combination except limonene + OH, at least one isomer can be found for which the
30
31 332 Gibbs energy of reaction 2 is around or below -4 kcal/mol.

333

334 Intra-molecular hydrogen bonds generally lower the Gibbs energy of molecules. A lower
335 reactant RO_2 energy (for example, due to hydrogen bonding) will increase the reaction energy,
336 while a lower product RO energy will decrease the reaction energy. The alkoxy RO product
337 from the OH-oxidized RO_2 isomer for α -pinene shown in Table 1 has the alkoxy oxygen on the
338 opposite side of the ring to the OH-group and is therefore unable to form an intra-molecular
339 hydrogen bond. The RO_2 group in the reactant is more flexible and is able to form a weak
340 hydrogen bond with the OH group. This results in a high reaction 2 Gibbs energy of -0.12
341 kcal/mol. The reaction Gibbs energy corresponding to the reactant RO_2 isomer where the
342 OH-group is on the same side as the peroxy radical is significantly more exergonic (-6.40
343 kcal/mol) due to a strong intra-molecular hydrogen bond between the alkoxy oxygen and the
344 OH group in the product, and a relatively weaker interaction between the RO_2 group and

1
2
3
345 the OH group in the reactant. Figure 5 shows the two alkoxy radical isomers schematically.
4
5
346 Isomer b in the figure can form an intra-molecular hydrogen bond between the alkoxy-oxygen
6
7
347 and the OH-group and is consequently about 5 kcal/mol lower in Gibbs energy than the RO
8
9
348 isomer a.



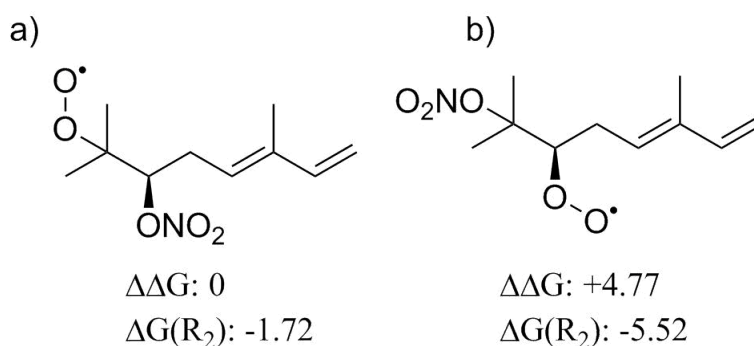
29
30
31
32
33
34
35
36
37
38
39
40
41
42
43
44
45
46
47
48
49
50
51
52
53
54
55
56
57
58
59
60

Figure 5: Alkoxy products of OH-oxidized α -pinene a) OH down, O up, b) OH down, O down. $\Delta\Delta G$ denotes the relative Gibbs energies of the alkoxy isomers and $\Delta G(R_2)$ is the Gibbs energy of reaction 2 producing this product. All values are in kcal/mol.

349 In the case of OH-derived RO_2 , the reaction rate may ultimately be controlled by the
350 degree of hydrogen bonding stabilization of the transition states, which cannot be directly
351 deduced from the overall reaction energies. In other words, our "rule of thumb" of an overall
352 reaction Gibbs energy not much above -4 kcal/mol being necessary for an efficient reaction 2
353 may have the largest uncertainty for the OH-oxidized cases.

354
355 In the case of NO_3 oxidation, the difference between the reaction Gibbs energies of dif-
356 ferent isomers for each monoterpene is controlled mainly by the stability of the reactant RO_2 ,
357 as the differences in Gibbs energies between the RO_2 isomers is larger than the difference in Gibbs
358 energies of the corresponding RO. For trans- β -ocimene, the most energetically favorable RO_2
359 isomer (shown in Table 2) was 3.68 kcal/mol lower in Gibbs energy than the next best RO_2

1
2
3
4 360 isomer. This showed in the reaction Gibbs energies for reaction 2, where the most favorable
5
6 361 RO₂ isomer lead to the highest (least negative) reaction Gibbs energy. The RO₂ isomer that
7
8 362 has the O₂ and ONO₂ functional groups in opposite positions compared to the lowest Gibbs
9
10 363 energy RO₂ isomer had a relative Gibbs energy of 4.77 kcal/mol and a reaction 2 Gibbs
11
12 364 energy of -5.52 kcal/mol. The two isomers are shown schematically in Figure 6. Similarly, the
13
14 365 Δ₃-carene NO₃ oxidized RO₂ isomer that is 2.60 kcal/mol (**b** in Figure 7) higher in Gibbs
15
16 366 energy than the most energetically favorable isomer (**a** in Figure 7) has a reaction 2 Gibbs
17
18 367 energy of -5.75 kcal/mol compared to -2.13 kcal/mol for the latter.



32
33
34
35
36
37
38
39
40
41
42
43
44
45
46
47
48
49
50
51
52
53
54
55
56
57
58
59
60

Figure 6: Two of the RO₂ isomers for NO₃ oxidized trans-β-ocimene that were studied. ΔΔG denotes the relative Gibbs energy in kcal/mol. **a**) Is the most energetically favorable RO₂ isomer, while **b**) is an isomer that is 4.77 kcal/mol higher in Gibbs energy. ΔG(R₂) is the Gibbs energy of reaction 2 involving this reactant.

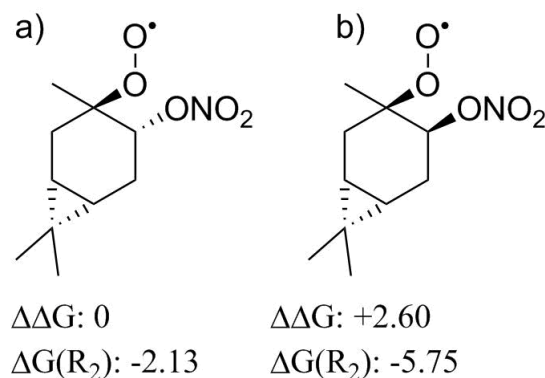


Figure 7: Two of the RO₂ isomers for NO₃ oxidized Δ₃-carene that were studied. ΔΔG denotes the relative Gibbs energy in kcal/mol. **a)** Is the most energetically favorable RO₂ isomer and **b)** is an isomer that is 3.25 kcal/mol higher in Gibbs energy. ΔG(R₂) is the Gibbs energy of reaction 2 involving this reactant.

24
25
26
27
28
29
30
31
32
33
34
35
36
37
38
39
40
41
42
43
44
45
46
47
48
49
50
51
52
53
54
55
56
57
58
59
60

368 The Gibbs energies of reaction 2 for the O₃ oxidized systems were on average slightly
369 lower than for the OH and NO₃-oxidized cases. The variation of Gibbs energies (both for
370 different RO₂ isomers from the same monoterpene, and between monoterpenes) was also
371 generally slightly smaller, possibly due to weaker direct interactions between the carbonyl
372 group and the radical centers compared to the ONO₂ or OH cases. Crucially, most RO₂
373 isomers derived from O₃ oxidation of monoterpenes had Gibbs energies just around or below
374 -4 kcal/mol for reaction 2, implying that they could be competitive in the atmosphere. The
375 main exceptions to this trend are some RO₂ isomers from trans-β-ocimene and Δ³-carene
376 ozonolysis, which have reaction Gibbs energies between -2 and -3 kcal/mol, and one of the
377 RO₂ isomers from β-pinene ozonolysis, which has an anomalously low reaction Gibbs energy of
378 -7.16 kcal/mol. This last isomer has the RO₂ (and subsequent RO) group located on a tertiary
379 carbon atom, leading to an exceptionally low energy for the RO product. While spontaneous
380 breaking of the cyclo-butyl ring by the oxy-radical on the tertiary carbon was expected (and
381 was observed at the lower-level B3LYP/6-31+G* optimization), a direct optimization at
382 the higher ωB97X-D/aug-cc-pVTZ level found an alkoxy radical minimum (note that the
383 ring-breaking reaction is still likely to have a low barrier, and occur before any other reaction
384 in atmospheric conditions). The three RO isomers of ozone oxidized β-pinene along with the

385 difference in relative Gibbs energies are shown in Figure 8. It should be noted that isomer
 386 **a** is unlikely to form in the atmosphere as the initial hydrogen abstraction by the Criegee
 387 intermediate required to form the preceding RO₂ has a barrier of 25 kcal/mol.⁵⁹

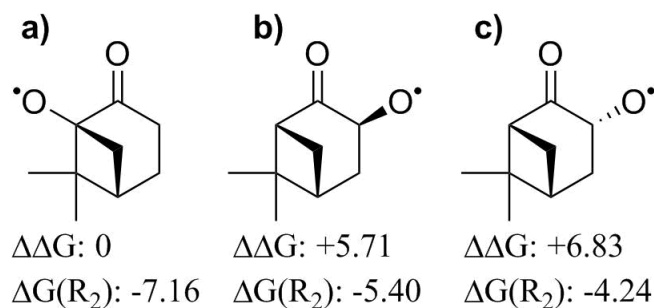
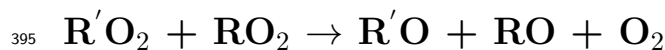


Figure 8: The three RO isomers for O₃ oxidized β -pinene. $\Delta\Delta G$ denotes the relative Gibbs energy in kcal/mol. **a)** Is the isomer with the oxy radical on the tertiary carbon atom, while **b)** and **c)** are the isomers with the oxy radical on the secondary carbon atom. $\Delta G(R_2)$ is the Gibbs energy of reaction 2 producing this product.

388 Reaction 3 was found to be consistently exergonic, by -13 to -25 kcal/mol, see Table S1
 389 in the SI for full details. The most favorable reaction Gibbs energies were observed for the
 390 isomers where the alcohol product formed an intra-molecular hydrogen bond with the O-atom
 391 of the OH, NO₃, and the carbonyl O functional groups from the three different oxidized
 392 systems, respectively. If (likely catalytic) kinetically competitive reaction mechanisms exist
 393 for reaction 3 also for the non-acyl peroxy radicals studied here, then thermodynamic factors
 394 will not prevent the reaction from occurring.



396 The mechanism of reaction 5 is currently uncertain. The most recent and theoretically rigor-
 397 ous computational study by Lee et al.⁵⁴ proposes (in agreement with a multireference study
 398 by Ghigo et al. from 2003⁶⁰) that all RO₂ + RO₂ reactions proceed via an RO...O₂...RO
 399 complex, where the two RO are coupled as a triplet, coupling to the triplet O₂ to give
 400 an overall singlet. Branching between the three different pathways (reactions 4, 5 and 6)

1
2
3
4 401 is then controlled by a competition between hydrogen abstraction, fragmentation of the
5
6 402 complex and intersystem crossing (and subsequent barrierless recombination of the two
7
8 403 RO), respectively. The thermodynamic parameters computed here can thus not be used
9
10 404 to assess relative probabilities of reaction 5 compared to the two other channels. However,
11
12 405 analogous to reaction 2, the $\text{RO}\cdots\text{O}_2\cdots\text{RO}$ complex also suffers from an entropy penalty to
13
14 406 its Gibbs energy compared to the separated products (in terms of the $-T\Delta S$ contribution
15
16 407 to the Gibbs energy at 298 K). For example, the entropy contribution to the Gibbs energy
17
18 408 of the $\text{CH}_3\text{CH}_2\text{O}\cdots\text{O}_2\cdots\text{OCH}_2\text{CH}_3$ complex was found to be 17 kcal/mol relative to the
19
20 409 separated products (calculated at M11//6-31+G(d,p) level employed by Lee et al.⁵⁴). Since
21
22 410 the entropy penalty to the Gibbs energy of the $\text{RO}\cdots\text{O}_2\cdots\text{OR}$ complex and the transition
23
24 411 state (or states) associated with its formation are likely quite similar (see Figure 4 **b** for the
25
26 412 analogous case for reaction 2), the overall $\text{RO}_2 + \text{RO}_2$ reaction is thus associated with a
27
28 413 Gibbs energy barrier around 17 kcal/mol higher than the reaction Gibbs energy computed
29
30 414 here, plus or minus any stabilizing or destabilizing enthalpic contributions, for example from
31
32 415 H-bonding or bond-breaking (respectively). Lee et al.⁵⁴ suggest (based on CCSD(T) energy
33
34 416 corrections) that the rate-limiting transition state for the $\text{CH}_3\text{CH}_2\text{OO} + \text{CH}_3\text{CH}_2\text{OO}$ reaction
35
36 417 is almost 13 kcal/mol above the $\text{RO}\cdots\text{O}_2\cdots\text{OR}$ complex in enthalpy. This would lead to
37
38 418 negligibly low overall reaction rates for the gas-phase $\text{CH}_3\text{CH}_2\text{OO} + \text{CH}_3\text{CH}_2\text{OO}$ reaction, in
39
40 419 disagreement with observations.¹⁷ CASPT2 calculations by Ghigo et al.⁶⁰ for the $\text{CH}_3\text{OO} +$
41
42 420 CH_3OO system suggest that the rate-limiting transition state is less than 2 kcal/mol above
43
44 421 the complex in enthalpy, leading to much better agreement with experiments. Here, we use
45
46 422 computed properties for a few model $\text{RO}\cdots\text{O}_2\cdots\text{OR}$ and $\text{RO}\cdots\text{OR}$ complexes, together
47
48 423 with our computed overall reaction Gibbs energies, to estimate lower limits for the barrier
49
50 424 heights for the $\text{RO}_2 + \text{RO}_2$ reactions. If the rate-limiting transition states are much higher
51
52 425 in enthalpy than the $\text{RO}\cdots\text{O}_2\cdots\text{OR}$ complex, the barriers would be correspondingly higher.
53
54 426 However, as long as the reaction proceeds via the $\text{RO}\cdots\text{O}_2\cdots\text{OR}$ complex, the rate-limiting
55
56 427 barrier cannot not be lower than the free energy of the complex.

428

1
2
3
4
5 429 If we consider that the stabilization of the $\text{RO}\cdots\text{O}_2\cdots\text{OR}$ complex is mostly from the
6
7 430 favorable interaction of the two RO, we can estimate this stabilization by looking at the
8
9 431 binding energy of $\text{RO}\cdots\text{RO}$. We considered a simple two-carbon model ROs for each of the
10
11 432 OH-, NO_3 , and O_3 -oxidized system. The calculation was done for an overall triplet state, as
12
13 433 the Lee et al.⁵⁴ mechanism indicates the two RO are initially coupled as a triplet (and ROOR
14
15 434 formation from two RO likely occurs spontaneously on the singlet surface). The binding
16
17 435 enthalpy (at the DLPNO/def2-QZVPP// ω B97X-D/aug-cc-pVTZ level of theory) for the
18
19 436 OH-, NO_3 - and O_3 oxidized $\text{RO}\cdots\text{RO}$ is 4.4, 3.9 and 2.7 kcal/mol, respectively. Considering
20
21 437 an entropy penalty to the transition state Gibbs energy of around 17 kcal/mol, a stabilization
22
23 438 of around 4 kcal/mol would mean that the rate limiting transition state (or intermediate) for
24
25 439 reaction 5 is at least around 13 kcal/mol above the separated products. For example, for a
26
27 440 reaction Gibbs energy of around -10 kcal/mol (implying that the products are 10 kcal/mol
28
29 441 below the reactants), the transition state would then be about 3 kcal/mol in Gibbs energy
30
31 442 above the reactants.

443

32
33
34
35 444 The reaction Gibbs energies of reaction 5 showed that the reaction was less favorable
36
37 445 when one of the reacting peroxy radicals was the OH-oxidized α -pinene isomer with the RO_2
38
39 446 functional group and the OH functional group on the opposite sides of the ring (see rows
40
41 447 **a** to **f** in Table 5). This is due to the previously discussed stabilization of the OH-oxidized
42
43 448 α -pinene RO_2 by a weak H-bond between the hydrogen atom of the OH group and the
44
45 449 RO_2 group and the absence of such an interaction in the corresponding RO product (see
46
47 450 Figure 9). For the reactions in the range of -5 to -10 kcal/mol, the lowering of the OH-oxidized
48
49 451 α -pinene peroxy radical isomer due to the interaction between the RO_2 and OH groups were
50
51 452 compensated by the relatively high energies of the second RO_2 reactant in the reaction. The
52
53 453 NO_3 -oxidized trans- β -ocimene RO_2 isomer in row **d** in Table 5 is 4.4 kcal/mol higher in
54
55 454 Gibbs energy compared to the most favorable NO_3 -oxidized trans- β -ocimene RO_2 isomer.

1
2
3
4 455 Similarly, the OH-oxidized β -pinene RO₂ in row **e** in the table has the peroxy radical group
5
6 456 on a secondary carbon, and is consequently 1 kcal/mol higher in Gibbs energy relative to the
7
8 457 lowest energy OH-oxidized β -pinene RO₂ isomer. While 1 kcal/mol should not significantly
9
10 458 affect the overall reaction Gibbs energy on its own, the ΔG is augmented by the low energy
11
12 459 of the corresponding RO product of this OH-oxidized β -pinene RO₂ isomer in row **e**, which
13
14 460 is the most favorable RO isomer of the four considered in this study. For the third case in
15
16 461 this energy range, the ΔG is significantly influenced by the previously discussed low RO
17
18 462 Gibbs energy of the O₃-oxidized β -pinene isomer in row **f** in Table 5. In the -10 to -17
19
20 463 kcal/mol energy range in Table 5, the NO₃-oxidized α -pinene R'O₂ and OH-oxidized β -pinene
21
22 464 RO₂ in row **g** are both less favorable isomers (2.8 kcal/mol and 2 kcal/mol higher than
23
24 465 the most favorable NO₃-oxidized α -pinene and OH-oxidized- β -pinene RO₂s, respectively),
25
26 466 translating to lower overall ΔG s. In row **h**, in addition to the OH-oxidized α -pinene and
27
28 467 NO₃-oxidized Δ^3 -carene being unfavorable by 1.4 and 2.6 kcal/mol, respectively, relative to
29
30 468 their corresponding most favorable RO₂ isomer, the low ΔG can be explained by the low
31
32 469 energy of the RO products of the two isomers (the lowest energy OH-oxidized RO isomer in
33
34 470 the α -pinene case, and only 0.3 kcal/mol higher than the lowest energy NO₃ oxidized RO
35
36 471 isomer in the Δ^3 -carene case). Finally, the lowest ΔG was found for the reaction between
37
38 472 the two O₃-oxidized β -pinene RO₂s (row **i**) due to the low energy of the corresponding RO
39
40 473 product.

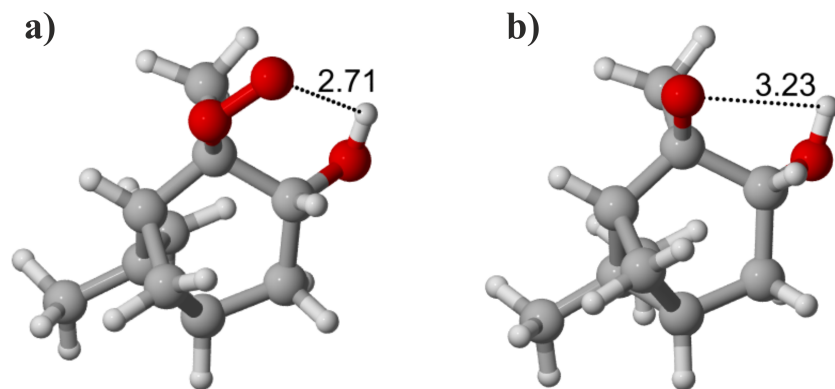


Figure 9: Distances between the OH group and the RO₂ group (a) and the OH group and the RO group (b). The interaction between the OH group and the RO₂ group in (a) translates to a lower RO₂ energy.

Conclusion

Multiple channels compete for RO₂ + HO₂ and RO₂ + RO₂ reactions. The thermodynamics of the two radical propagation reactions involving monoterpene derived RO₂s were studied here. This is the first time such a study has been carried out for a large set of atmospherically relevant monoterpenes and oxidants. The reaction Gibbs energies were exergonic for all cases. However, the RO₂ + HO₂ → RO + OH + O₂ channel (reaction 2) was found to be only barely so for some of the OH and the NO₃ oxidized systems, especially for the lowest-energy RO₂ isomers. Using our simple "rule of thumb" that the reaction Gibbs energy cannot be much higher than -4 kcal/mol for reaction 2 to be competitive, we can rule out this reaction for most OH and NO₃-derived first generation monoterpene RO₂ isomers. However, for each monoterpene-oxidant combination except limonene + OH, at least one RO₂ isomer can be found for which the Gibbs energy of reaction 2 is around or below -4 kcal/mol. These RO₂ isomers could thus conceivably have non-negligible yields for reaction 2. The ozone-derived RO₂s, especially from β-pinene, have somewhat lower reaction Gibbs energies, and for many of their isomers reaction 2 may be feasible.

1
2
3
4 490 The $R'O_2 + RO_2 \rightarrow R'O + RO + O_2$ reaction (reaction 5) Gibbs energies varied from
5
6 491 a maximum of ~ -3 kcal/mol for the α -pinene-OH system to a minimum of ~ -17 kcal/mol for
7
8 492 the β -pinene- O_3 system. The structure of the reactant RO_2 and the product RO strongly
9
10 493 affect the reaction Gibbs energies. $RO_2 + RO_2$ self-reaction rates as low as 3×10^{-17} cm³
11
12 494 molecule⁻¹ s⁻¹ have been observed for systems similar to those studied here (tertiary C₄H₉O₂
13
14 495 radical, in this case).⁶¹ Assuming that the overall mechanism proposed by Ghigo et al.⁶⁰ and
15
16 496 Lee et al.⁵⁴ for $RO_2 + RO_2$ reactions is correct, all RO_2 s studied here should have self-reaction
17
18 497 rates faster than the slowest observed rate. We can qualitatively conclude, however, that O_3 -
19
20 498 derived monoterpene RO_2 are generally likely to have higher, and OH-derived RO_2 lower,
21
22 499 overall self- and cross-reaction rates, with NO_3 -derived RO_2 representing an intermediate
23
24 500 case between the other two.

501 Supporting information

502 The Supporting Information is available free of charge via the Internet at <http://pubs.acs.org/>
503 and includes reaction Gibbs energies for the studied reactions for all isomers. Output files
504 (.log and .out) for all studied systems are provided in a zip file archived at:
505 <https://doi.org/10.5281/zenodo.1476995>

506 Acknowledgements

507 SI, HR, MPR and TK thank the Academy of Finland (266388,299574), and KHM and HGK
508 thank the Danish Center for Scientific Computing for the financial support. We also thank
509 the CSC IT Center for Science in Espoo, Finland for computing resources.

510 **References**

- 511 (1) Ehn, M.; Thornton, J. A.; Kleist, E.; Sipilä, M.; Junninen, H.; Pullinen, I.; Springer, M.;
512 Rubach, F.; Tillmann, R.; Lee, B.; et al. A Large Source of Low-Volatility Secondary
513 Organic Aerosol. *Nature* **2014**, *506*, 476-479.
- 514 (2) Mentel, T. F.; Springer, M.; Ehn, M.; Kleist, E.; Pullinen, I.; Kurtén, T.; Rissanen,
515 M.; Wahner, A.; Wildt, J. Formation of Highly Oxidized Multifunctional Compounds:
516 Autoxidation of Peroxy Radicals Formed in the Ozonolysis of Alkenes - Deduced from
517 Structure-Product Relationships. *Atmos. Chem. Phys.* **2015**, *15*, 6745-6765.
- 518 (3) Berndt, T.; Richters, S.; Kaethner, R.; Voigtländer, J.; Stratmann, F.; Sipilä, M.;
519 Kulmala, M.; Herrmann, H. Gas-Phase Ozonolysis of Cycloalkenes: Formation of Highly
520 Oxidized RO₂ Radicals and Their Reactions With NO, NO₂, SO₂, and Other RO₂
521 Radicals. *J. Phys. Chem. A* **2015**, *41*, 10336-10348.
- 522 (4) Rissanen, M. P.; Kurtén, T.; Sipilä, M.; Thornton, J. A.; Kangasluoma, J.; Sarnela,
523 N.; Junninen, H.; Jørgensen, S.; Schallhart, S.; Kajos, M. K.; et al. The Formation of
524 Highly Oxidized Multifunctional Products in the Ozonolysis of Cyclohexene. *J. Am.*
525 *Chem. Soc.* **2014**, *136*, 15596-15606.
- 526 (5) IPCC, 2013: Climate Change 2013: The Physical Science Basis. Contribution of Working
527 Group I to the Fifth Assessment Report of the Intergovernmental Panel on Climate
528 Change [Stocker, T.F., D. Qin, G.-K. Plattner, M. Tignor, S.K. Allen, J. Boschung, A.
529 Nauels, Y. Xia, V. Bex, P.M. Midgley (eds.)]. Cambridge University Press, Cambridge,
530 United Kingdom and New York, NY, USA, 1535 pp, doi:10.1017/CBO9781107415324.
- 531 (6) Sindelarova, K.; Granier, C.; Bouarar, I.; Guenther, A.; Tilmes, S.; Stavrakou, T.;
532 Müller, J.-F.; Kuhn, U.; Stefani, P.; Knorr, W. Global Data Set of Biogenic VOC
533 Emissions Calculated by the MEGAN Model Over the Last 30 Years. *Atmos. Chem.*
534 *Phys.* **2014**, *14*, 9317-9341.

- 1
2
3
4 535 (7) Crounse, J. D.; Nielsen, L. B.; Jørgensen, S.; Kjaergaard, H. G.; Wennberg, P. O.
5
6 536 Autoxidation of Organic Compounds in the Atmosphere. *J. Phys. Chem. Lett.* **2013**, *4*,
7
8 537 3513-3520.
9
- 10 538 (8) Kurtén, T.; Rissanen, M. P.; Mackeprang, K.; Thornton, J. A.; Hyttinen, N.; Jørgensen,
11
12 539 S.; Ehn, M.; Kjaergaard, H. G. Computational Study of Hydrogen Shifts and Ring-
13
14 540 Opening Mechanisms in α -Pinene Ozonolysis Products. *J. Phys. Chem. A* **2015**, *119*,
15
16 541 11366-11375.
17
- 18 542 (9) Atkinson, R. Gas-Phase Tropospheric Chemistry of Volatile Organic Compounds: 1.
19
20 543 Alkanes and Alkenes. *J. Phys. Chem. Ref. Data* **1997**, *26*, 215-290.
21
22
- 23 544 (10) Park, J.; Jongsma, C. G.; Zhang, R.; North, S. W. OH/OD Initiated Oxidation of
24
25 545 Isoprene in the Presence of O₂ and NO. *J. Phys. Chem. A* **2004**, *108*, 10688-10697.
26
27
- 28 546 (11) Cabañas, B.; Salgado, S.; Ballesteros, B.; Martínez, E. An Experimental Study on the
29
30 547 Temperature Dependence for the Gas-Phase Reactions of NO₃ Radical with a Series of
31
32 548 Aliphatic Aldehydes. *J. Atmos. Chem.* **2001**, *40*, 23-39.
33
34
- 35 549 (12) Doussin, J. F.; Picquet-Varrault, B.; Durand-Jolibois, R.; Loirat, H.; Carlier, P. A
36
37 550 Visible and FTIR Spectrometric Study of the Nighttime Chemistry of Acetaldehyde
38
39 551 and PAN Under Simulated Atmospheric Conditions. *J. Photochem. Photobio. A* **2003**,
40
41 552 *157*, 283-293.
42
- 43 553 (13) Ng, N. L.; Brown, S. S.; Archibald, A. T.; Atlas, E.; Cohen, R. C.; Crowley, J. N.; Day,
44
45 554 D. A.; Donahue, N. M.; Fry, J. L.; Fuchs, H. F.; et al. Nitrate Radicals and Biogenic
46
47 555 Volatile Organic Compounds: Oxidation, Mechanisms, and Organic Aerosol. *Atmos.*
48
49 556 *Chem. Phys.* **2017**, *17*, 2103-2162.
50
51
- 52 557 (14) Day, D. A.; Liu, S.; Russell, L. M.; Ziemann, P. J. Organonitrate Group Concentrations
53
54 558 in Submicron Particles With High Nitrate and Organic Fractions in Coastal Southern
55
56 559 California. *Atmos. Env.* **2010**, *44*, 1970-1979.
57
58
59
60

- 1
2
3
4 560 (15) Lee, B. H.; Mohr, C.; Lopez-Hilfiker, F. D.; Lutz, A.; Hallquist, M.; Lee, L.; Romer,
5
6 561 P.; Cohen, R. C.; Iyer, S.; Kurtén, T.; et al. Highly Functionalized Organic Nitrates in
7
8 562 the Southeast United States: Contribution to Secondary Organic Aerosol and Reactive
9
10 563 Nitrogen Budgets. *P. Natl. Acad. Sci.* **2016**, *113*, 1516-1521.
- 11
12 564 (16) Monge-Palcious, M.; Rissanen, M. P.; Wang, Z.; Sarathy, S. M. Theoretical Kinetic
13
14 565 Study of the Formic Acid Catalyzed Criegee Intermediate Isomerization: Multistructural
15
16 566 Anharmonicity and Atmospheric Implications. *Phys. Chem. Chem. Phys.* **2018**, *20*,
17
18 567 10806-10814.
- 19
20
21 568 (17) Orlando, J. J.; Tyndall, G. S. Laboratory Studies of Organic Peroxy Radical Chemistry:
22
23 569 An Overview with Emphasis on Recent Issues of Atmospheric Significance. *Chem. Soc.*
24
25 570 *Rev.* **2012**, *41*, 6294-6317.
- 26
27
28 571 (18) Orlando, J. J.; Tyndall, G. S.; Wallington, T. J. The Atmospheric Chemistry of Alkoxy
29
30 572 Radicals. *Chem. Rev.* **2003**, *103*, 4657-4689.
- 31
32 573 (19) Hasson, A. S.; Tyndall, G. S.; Orlando, J. J.; Singh, S.; Hernandez, S. Q.; Cambell, S.;
33
34 574 Ibarra, Y. Branching Ratios For the Reaction of Selected Carbonyl-Containing Peroxy
35
36 575 Radicals With Hydroperoxy Radicals. *J. Phys. Chem. A* **2012**, *116*, 6264-6281.
- 37
38
39 576 (20) Vereecken, L.; Peeters, J. Decomposition of Substituted Alkoxy Radicals - Part I: A
40
41 577 Generalized Structure-Activity Relationship for Reaction Barrier Heights. *Phys. Chem.*
42
43 578 *Chem. Phys.* **2009**, *11*, 9062-9074.
- 44
45
46 579 (21) Dames, E. E.; Green, W. H. The Effect of Alcohol and Carbonyl Functional Groups on
47
48 580 the Competition between Unimolecular Decomposition and Isomerization in C₄ and C₅
49
50 581 Alkoxy Radicals. *Int. J. Chem. Kinet.* **2016**, *48*, 544-555.
- 51
52 582 (22) Hasson, A. S.; Tyndall, G. S.; Orlando, J. J. A Product Yield Study of the Reaction o
53
54 583 HO₂ Radicals with Ethyl Peroxy (C₂H₅O₂), Acetyl Peroxy (CH₃C(O)O₂), and Acetonyl
55
56 584 Peroxy (CH₃C(O)CH₂O₂) Radicals. *J. Phys. Chem. A* **2004**, *108*, 5979-5989.

- 1
2
3
4 585 (23) Hasson, A. S.; Kuwata, K. T.; Arroyo, M. C.; Petersen, E. B. Theoretical Studies of
5
6 586 the Reaction of Hydroperoxy Radicals (HO_2) With Ethyl Peroxy ($\text{CH}_3\text{CH}_2\text{O}_2$), Acetyl
7
8 587 Peroxy ($\text{CH}_3\text{C}(\text{O})\text{O}_2$), and Acetonyl Peroxy ($\text{CH}_3\text{C}(\text{O})\text{CH}_2\text{O}_2$) Radicals. *J. Photochem.*
9
10 588 *Photobiol. A* **2005**, *176*, 218-230.
- 11
12 589 (24) Jokinen, T.; Berndt, T.; Makkonen, R.; Kerminen V. -M.; Junninen, H.; Paasonen P.;
13
14 590 Stratmann, F.; Herrmann, H.; Guenther, A. B.; Worsnop, D. R. et al. Production of
15
16 591 Extremely Low Volatile Organic Compounds from Biogenic Emissions: Measured Yields
17
18 592 and Atmospheric Implications. *Proc. Natl. Acad. Sci.* **2015**, *112*, 7123-7128.
- 19
20
21 593 (25) Iyer, S.; He, X.; Hyttinen, N.; Kurtén, T.; Rissanen, M. Computational and Experimental
22
23 594 Investigation of the Detection of HO_2 Radical and the Products of Its Reaction with
24
25 595 Cyclohexene Ozonolysis Derived RO_2 Radicals by an Iodide-Based Chemical Ionization
26
27 596 Mass Spectrometer. *J. Phys. Chem. A* **2017**, *121*, 6778-6789.
- 28
29
30 597 (26) Hyttinen, N.; Knap, H. C.; Rissanen, M. P.; Jørgensen, S.; Kjaergaard, H. G.; Kurtén,
31
32 598 T. Unimolecular HO_2 Loss from Peroxy Radicals Formed in Autoxidation Is Unlikely
33
34 599 under Atmospheric Conditions. *J. Phys. Chem. A* **2016**, *120*, 3588-3595.
- 35
36
37 600 (27) Halgren, T. A. Merck Molecular Force Field. I. Basis, Form, Scope, Parameterization,
38
39 601 and Performance of MMFF94. *J. Comput. Chem.* **1996**, *17*, 490-519.
- 40
41
42 602 (28) Halgren, T. A. Merck Molecular Force Field. II. MMFF94 van der Waals and Electrostatic
43
44 603 Parameters for Intermolecular Interactions. *J. Comput. Chem.* **1996**, *17*, 520-552.
- 45
46
47 604 (29) Halgren, T. A. Merck Molecular Force Field. III. Molecular Geometries and Vibrational
48
49 605 Frequencies for MMFF94. *J. Comput. Chem.* **1996**, *17*, 553-586.
- 50
51
52 606 (30) Halgren, T. A.; Nachbar, R. B. Merck Molecular Force Field. IV. Conformational
53
54 607 Energies and Geometries for MMFF94. *J. Comput. Chem.* **1996**, *17*, 587-615.
- 55
56
57
58
59
60

- 1
2
3
4 608 (31) Halgren, T. A. Merck Molecular Force Field. V. Extension of MMFF94 Using Experi-
5
6 609 mental Data, Additional Computational Data, and Empirical Rules. *J. Comput. Chem.*
7
8 610 **1996**, *17*, 616-641.
- 9
10 611 (32) Halgren, T. A. MMFF VII. Characterization of MMFF94, MMFF94s, and Other Widely
11
12 612 Available Force Fields for Conformational Energies and for Intermolecular-Interaction
13
14 613 Energies and Geometries. *J. Comput. Chem.* **1999**, *20*, 730-748.
- 15
16
17 614 (33) Becke, A. D. Density-Functional Thermochemistry. III. The Role of Exact Exchange. *J.*
18
19 615 *Chem. Phys.* **1993**, *98*, 5648-5652.
- 20
21
22 616 (34) Lee, C.; Yang, W.; Parr, R. H. Development of the Colle-Salvetti Correlation-Energy
23
24 617 Formula Into a Functional of the Electron Density. *Phys. Rev. B* **1988**, *37*, 785-789.
- 25
26
27 618 (35) Hehre, W. J.; Ditchfield, R.; Pople, J. A. Self-Consistent Molecular Orbital Methods.
28
29 619 XII. Further Extensions of Gaussian-Type Basis Sets for Use in Molecular Orbital
30
31 620 Studies of Organic Molecules. *J. Chem. Phys.* **1972**, *56*, 2257-2261.
- 32
33
34 621 (36) Clark, T.; Jayaraman, C.; Spitznagel, G. W.; Schleyer, P. v. R. Efficient Diffuse Function-
35
36 622 Augmented Basis Sets for Anion Calculations. III. The 3-21+G Basis Set for First-Row
37
38 623 Elements, Li-F. *J. Comput. Chem.* **1983**, *4*, 294-301.
- 39
40 624 (37) Frisch, M. J.; Pople, J. A.; Stephen, B. J. Self-Consistent Molecular Orbital Methods 25.
41
42 625 Supplementary Functions for Gaussian Basis Sets. *J. Chem. Phys.* **1984**, *80*, 3265-3269.
- 43
44
45 626 (38) Møller, K. H.; Otkjaer, R. V.; Hyttinen, N.; Kurtén, T.; Kjaergaard, H. G. Cost-Effective
46
47 627 Implementation of Multiconformer Transition State Theory for Peroxy Radical Hydrogen
48
49 628 Shift Reactions. *J. Phys. Chem. A* **2016**, *120*, 10072-10087.
- 50
51
52 629 (39) Spartan '14; Wavefunction Inc: Irvine CA, 2014.
- 53
54
55 630 (40) Spartan '16; Wavefunction Inc: Irvine CA, 2016.
- 56
57
58
59
60

- 1
2
3
4 631 (41) Hyttinen, N.; Rissanen, M. P.; Kurtén, T. Computational Comparison of Acetate and
5
6 632 Nitrate Chemical Ionization of Highly Oxidized Cyclohexene Ozonolysis Intermediates
7
8 633 and Products. *J. Phys. Chem. A* **2017**, *121*, 2172-2179.
9
- 10 634 (42) Chai, J. D.; Head-Gordon, M. Long-Range Corrected Hybrid Density Functionals with
11
12 635 Damped Atom-Atom Dispersion Corrections. *Phys. Chem. Chem. Phys.* **2008**, *10*,
13
14 636 6615-6620.
15
- 16
17 637 (43) Dunning, T. H. Gaussian Basis Sets for Use in Correlated Molecular Calculations. I.
18
19 638 The Atoms Boron Through Neon and Hydrogen. *J. Chem. Phys.* 1989, *90*, 1007-1023.
20
- 21
22 639 (44) Kendall, R. A.; Dunning, T. H.; Harrison, R. J. Electron Affinities of the First-Row
23
24 640 Atoms Revisited. Systematic Basis Sets and Wave Functions. *J. Chem. Phys.* 1992, *96*,
25
26 641 6796-6806.
27
- 28
29 642 (45) Frisch, M. J.; Trucks, G. W.; Schlegel, H. B.; Scuseria, G. E.; Robb, M. A.; Cheeseman,
30
31 643 J. R.; Scalmani, G.; Barone, V.; Mennucci, B.; Petersson, G. A.; et al. *Gaussian 09*.
32
33 644 Revision D.01, Gaussian, Inc.: Wallingford, CT, 2009.
34
- 35
36 645 (46) Partanen, L.; Vehkamäki, H.; Hansen, K.; Elm, J.; Henschel, H.; Kurtén, T.; Halonen,
37
38 646 R.; Zapadinsky, E. Effect of Conformers on Free Energies of Atmospheric Complexes. *J.*
39
40 647 *Phys. Chem. A* **2016**, *120*, 8613-8624.
41
- 42
43 648 (47) Riplinger, C. Neese, F. An Efficient and Near Linear Scaling Pair Natural Orbital Based
44
45 649 Local Coupled Cluster Method. *J. Chem. Phys.* **2013**, *138*, 034106.
46
- 47
48 650 (48) Neese, F. The ORCA Program System. *Wiley Interdiscip. Rev. Comput. Mol. Sci.* **2012**,
49
50 651 *2*, 73-78.
51
- 52
53 652 (49) Minenkov, Y.; Wang, H.; Wang, Z.; Sarathy, S. M.; Cavallo, L. Heats of Formation of
54
55 653 Medium-Sized Organic Compounds from Contemporary Electronic Structure Methods.
56
57 654 *J. Chem. Theory Comput.* **2017**, *13*, 3537-3560.
58
59
60

- 1
2
3
4 655 (50) Montgomery, J. A. Jr.; Frisch, M. J. A Complete Basis Set Model Chemistry. VI. Use Of
5
6 656 Density Functional Geometries and Frequencies. *J. Chem. Phys.* **1999**, *110*, 2822-2827.
7
8
9 657 (51) Peverati, R.; Truhlar, D. G. Improving the Accuracy of Hybrid Meta-GGA Density
10
11 658 Functionals by Range Separation. *J. Phys. Chem. Lett.* **2011**, *2*, 2810-2817.
12
13 659 (52) Ditchfield, R.; Hehre, W. J.; Pople, J. A. Self-Consistent Molecular Orbital Methods. IX.
14
15 660 An Extended Gaussian-Type Basis for Molecular-Orbital Studies of Organic Molecules.
16
17 661 *J. Chem. Phys.* **1971**, *54*, 724-728.
18
19
20 662 (53) Hariharan, P. C.; Pople, J. A. The Influence of Polarization Functions on Molecular
21
22 663 Orbital Hydrogenation Energies. *Theor. Chem. Acc.* **1973**, *28*, 213-222.
23
24
25 664 (54) Lee, R.; Grynova, G.; Ingold, K. U.; Coote, M. L. Why Are Sec-Alkylperoxyl Bimolecular
26
27 665 Self-Reactions Orders of Magnitude Faster Than the Analogous Reactions of Tert-
28
29 666 Alkylperoxyls? The Unanticipated Role of CH Hydrogen Bond Donation. *Phys. Chem.*
30
31 667 *Chem. Phys.* **2016**, *18*, 23673.
32
33
34 668 (55) Rio, C.; Flaud, P.-M.; Loison, J.-C.; Villenave, E. Experimental Reevaluation of the
35
36 669 Importance of the Abstraction Channel in the Reactions of Monoterpenes with OH
37
38 670 Radicals. *Chem. Phys. Chem.* **2010**, *11*, 3962-3970.
39
40
41 671 (56) Atkinson, R.; Arey, J. Gas-Phase Tropospheric Chemistry of Biogenic Volatile Organic
42
43 672 Compounds: A Review. *Atmos. Environ.* **2003**, *37*, 197-219.
44
45
46 673 (57) Ham, J. E.; Harrison, J. C.; Jackson, S. R.; Wells, J. R. Limonene Ozonolysis in the
47
48 674 Presence of Nitric Oxide: Gas-Phase Reaction Products and Yields. *Atmos. Environ.*
49
50 675 **2016**, *132*, 300-308.
51
52 676 (58) Boyd, A. A.; Flaud, P.-M.; Daugey, N.; Lesclaux, R. Rate Constants for RO₂ + HO₂
53
54 677 Reactions Measured Under a Large Excess of HO₂. *J. Phys. Chem. A* **2003**, *6*, 818-821.
55
56
57
58
59
60

- 1
2
3
4 678 (59) Nguyen, T. L.; Peeters, J.; Vereecken, L. Theoretical Study of the Gas-Phase Ozonolysis
5
6 679 of β -Pinene ($C_{10}H_{16}$). *Phys. Chem. Chem. Phys.* **2009**, *11*, 5643-5656.
7
8 680 (60) Ghigo, G.; Maranzana, A.; Tonachini, G. Combustion and Atmospheric Oxidation of
9
10 681 Hydrocarbons: Theoretical Study of the Methyl Peroxyl Self-Reaction. *J. Chem. Phys.*
11
12 682 **2003**, *118*, 10575-10583.
13
14
15 683 (61) Shallcross, D. E.; Raventos-Duran, M. T.; Bardwell, M. W.; Bacak, A.; Solman, Z.;
16
17 684 Percival, C. J. A Semi-Emperical Correlation for the Rate Coefficients for Cross- and
18
19 685 Self-Reactions of Peroxy Radicals in the Gas-Phase. *Atmos. Env.* **2005**, *39*, 763-771.
20
21
22
23
24
25
26
27
28
29
30
31
32
33
34
35
36
37
38
39
40
41
42
43
44
45
46
47
48
49
50
51
52
53
54
55
56
57
58
59
60

686 TOC Graphic

